

Electron transport through ribbonlike molecular wires calculated using density-functional theory and Green's function formalism

D. Visontai, I. M. Grace, and C. J. Lambert

Department of Physics, Lancaster University, Lancaster LA1 4YB, United Kingdom

(Received 6 December 2009; published 8 January 2010)

We study the length dependence of electron transport through three families of rigid, ribbonlike molecular wires. These series of molecules, known as polyacene dithiolates, polyphenanthrene dithiolates, and polyfluorene dithiolates, represent the ultimate graphene nanoribbons. We find that acenes are the most attractive candidates for low-resistance molecular-scale wires because the low-bias conductance of the fluorene- and phenanthrene-based families is shown to decrease exponentially with length, with inverse decay lengths of $\beta=0.29 \text{ \AA}^{-1}$ and $\beta=0.37 \text{ \AA}^{-1}$, respectively. In contrast, the conductance of the acene-based series is found to oscillate with length due to quantum interference. The period of oscillation is determined by the Fermi wave vector of an infinite acene chain and is approximately 10 \AA . Details of the oscillations are sensitive to the position of thiol end groups and in the case of “para” end groups, the conductance is found initially to increase with length.

DOI: 10.1103/PhysRevB.81.035409

PACS number(s): 85.65.+h, 73.63.-b, 81.07.Nb, 85.35.-p

Carbon-based electronics is developing at an accelerating pace, in part driven by the desire to develop sub-10-nm electronics. On the one hand, measurement of the electrical properties of single molecules sandwiched between metal contacts has recently become an experimental reality^{1–11} and has allowed a range of fundamental issues to be addressed, such as geometry-controlled (Ref. 12) and conformation-controlled (Refs. 13–18) electron transport and single-molecule sensing.¹⁹ On the other hand, the recently discovered ability to isolate graphene flakes^{20–22} has generated an explosion of interest in top-down approaches to carbon-based nanoelectronics. In this paper, we examine the three families of molecules shown in Fig. 1, which sit at the boundary between these two approaches. These series of molecules, known as polyacene dithiolates, polyphenanthrene dithiolates, and polyfluorene dithiolates, represent the ultimate graphene nanoribbons. They are attractive from a single-molecule perspective because they are rigid structures and avoid complexities associated with ring rotations.^{13,14} Furthermore, in contrast with graphene ribbons, whose edges suffer from atomic-scale uncertainties and are therefore expected to exhibit Levy flights²³ rather than ballistic transport, these families of molecules have well-defined edges and therefore electron transport is potentially ballistic.

Early studies of the electronic structure of these molecules provide a foretaste of fundamental properties shared by graphene ribbons. For example, a theoretical prediction that polyacenes should exhibit interesting magnetic phases²⁴ was followed by a study of zigzag graphene ribbons, which predicted an antiferromagnetic ground state.²⁵ More recently, it was predicted that the ground state of acenes with eight or more phenyl rings should be antiferromagnetic with unpaired electrons of opposite spins localized on the edges of the molecules.^{26,27} The resulting polyradical is highly reactive, which is consistent with the fact that to date, acenes with eight or more fused rings have not been synthesized.

The aim of the present paper is to examine the electrical conductance of these molecules, attached by thiol anchor groups to gold electrodes. As emphasized in a recent experi-

mental study²⁸ of diaminoacenes, electrical conductance depends both on the electronic structure of the molecule and on the position of the anchor group. Therefore we present results for the acene family with two positions of the thiol anchor groups, namely, the “para” and “meta” positions indicated in Figs. 1(c) and 1(d).

The main results of our calculations are presented in Fig. 2, which shows the room-temperature, zero-bias conductance of the above families of molecules, with different numbers n of fused benzene rings and lengths up to 18 \AA . In contrast with a recent suggestion²⁹ that the low-bias conductance of para-acenes should decrease exponentially with length, Fig. 2 shows that for both the para- and meta-acene series, no such exponential dependence exists. Indeed in the case of the former, quantum interference initially causes the zero-bias conductance to increase with length. This result is consistent

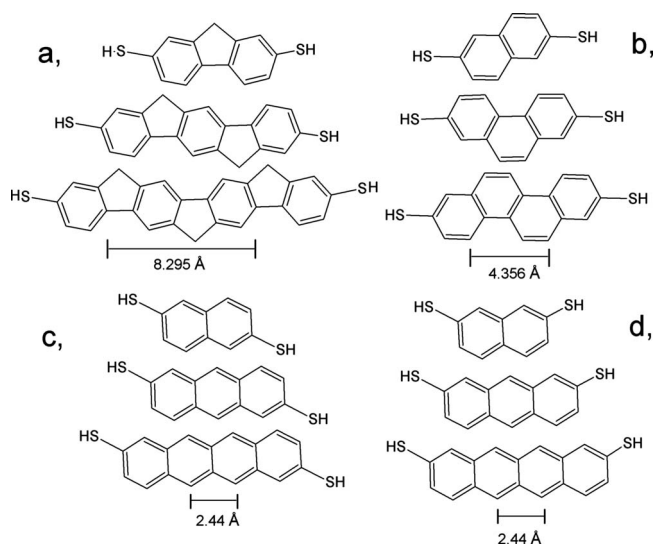


FIG. 1. The molecules: (a) fluorenes and (b) phenanthrenes, and two types of acenes, which we will call (c) para and (d) Meta. The molecules consist of $n=2, 3$, and 4 fused benzene rings. Length of unit cell: $a_{uc}=8.295 \text{ \AA}$, 4.3567 \AA , and 2.44 \AA .

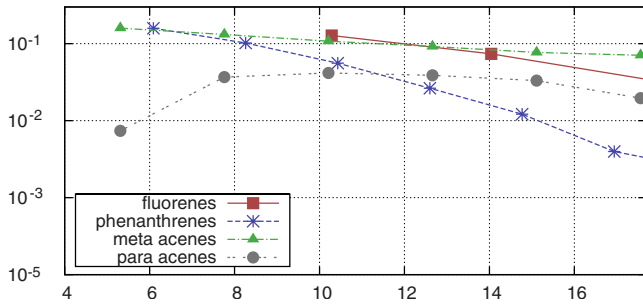


FIG. 2. (Color online) Length dependence of the room-temperature conductance. $\beta_{flu} = -0.29$ and $\beta_{phe} = -0.37$. The number of benzene rings n in fluorenes are [2:4], for phenanthrenes [2:6], and for the acenes are [2:7]. The 7-acene is the longest acene molecule that can be synthesized.

with a study of an infinite acene chain,²⁴ which predicts a vanishing band gap and metallic behavior.

To demonstrate that the initial increase in the conductance of the para-acenes is due to quantum interference, Fig. 3 shows results for much longer molecules. Since polyacenes with n greater than 7 do not exist and since we merely wish to illustrate the effect of quantum interference without changing the symmetry of the ground state, the results shown in Fig. 2 are for a nonmagnetic ground state only. They clearly demonstrate the presence of conductance oscillations in both the para- and meta-acene series. To estimate the period of these oscillations, one notes that the computed Fermi wave vector of the infinite acenes is $k_F = 0.615 \text{ \AA}^{-1}$ and using $2\pi/k_F = \Delta L = \lambda/2$ yields a period of 10.21 \AA .

The oscillatory behavior of acenes is analogous to conductance oscillations found in atomic wires³⁰⁻³⁷ and in carbon nanotubes,^{38,39} and is in marked contrast with the conductances of the fluorene and phenanthrene⁴⁰ series, which decay exponentially with length, with inverse decay lengths of $\beta = 0.29 \text{ \AA}^{-1}$ and $\beta = 0.37 \text{ \AA}^{-1}$, respectively. This suggests that polyacene dithiolates are the more attractive candidates for low-conductance molecular wires. Indeed, their computed Fermi velocity is approximately $c/300$, where c is the velocity of light and therefore, like graphene, they should exhibit a high-speed ambipolar field effect.

Having presented our main results, we now discuss details of the computational method, which uses a combination of the density-functional theory code SIESTA (Ref. 41) and a

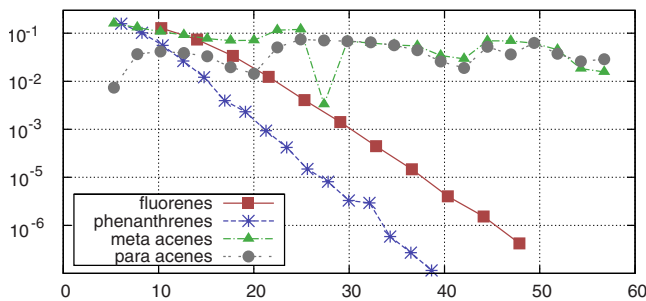


FIG. 3. (Color online) Length dependence of the room-temperature conductance. The number of benzene rings n in fluorenes are [2:12], for phenanthrenes [2:17], and for the acenes are [2:23].

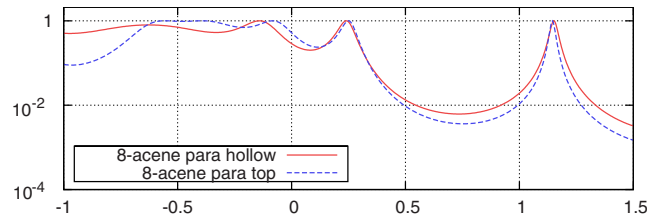


FIG. 4. (Color online) Comparison between hollow and top contacts.

Green's function scattering approach to calculate the transport.⁴² In these simulations the electronic and transport properties of the three families of molecules contacted between gold leads were calculated with the SMEAGOL code. SMEAGOL uses the Hamiltonian provided by SIESTA to obtain the electron transmission coefficients and here we focus on the zero-bias regime. The calculations used a double-zeta basis set to span the valence orbitals, an energy cutoff of 100 Ry to define the real-space grid and the local-density approximation (LDA) to calculate the exchange and correlation energy. The molecular coordinates were relaxed until all forces on the molecules were less than 0.02 eV/\AA and gold leads were added along the (111) direction to create the extended molecule. Here, nine atoms of gold per layer were used and five layers were enough to ensure the transmission coefficients were converged thus avoiding any spurious effects produced by the surfaces of the leads. The calculation was not spin polarized. Using Troullier-Martins pseudopotentials⁴³ and the Ceperley-Alder LDA (Ref. 44) to describe the exchange correlation of the underlying mean-field Hamiltonian, the zero-bias Green's function and scattering matrix are computed and from the latter one obtains the transmission coefficient $T(E)$ for electrons of energy E passing through the molecule from one gold lead to the other. The zero-bias, finite-temperature conductance is given by the Landauer formula: $G = 2e^2/h \int_{-\infty}^{\infty} dE T(E) [-df(E-E_F)/dE]$, where $f(E-E_F)$ is the Fermi function. Figure 4 shows an example of $T(E)$ calculated with hollow and top contact positions. As expected the hollow position shows a higher $T(E)$

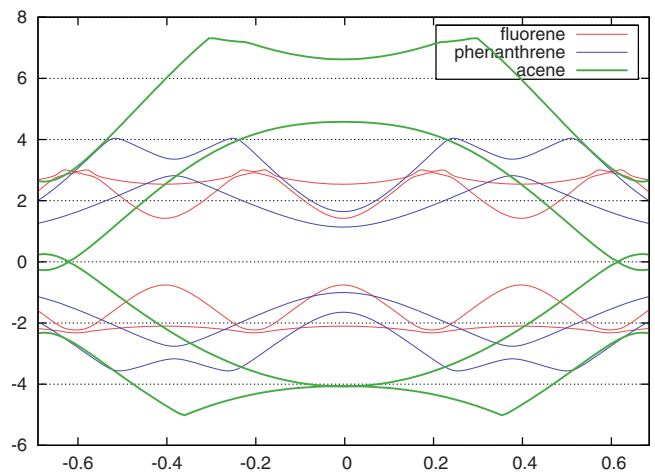


FIG. 5. (Color online) Band structure of infinite fluorene, acene, and phenanthrene as a function of the wave vector parallel to the backbone of the chains.

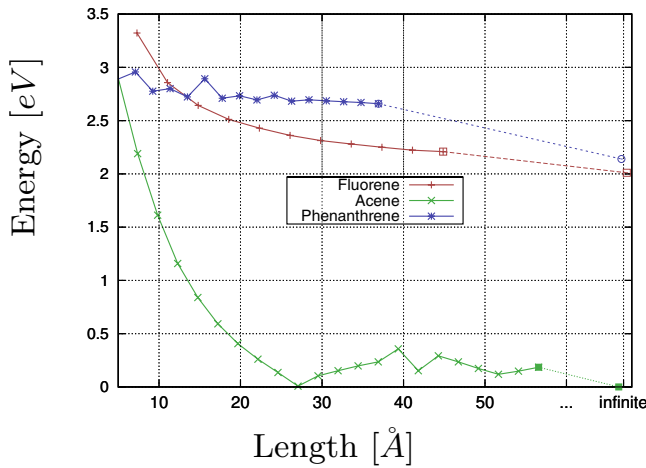


FIG. 6. (Color online) HL gaps of fluorenes, acenes, and phenanthrenes plotted as a function of the length of the molecules. The gaps for the infinitely long molecules is also shown.

in the HL gap because the S atom is closer to the surface of the Au lead and due to the stronger couplings the highest occupied molecular orbital (HOMO) resonance is broader. In this paper, we show results corresponding to hollow contacts only and choose the energy origin to correspond to the Fermi energy of the gold electrodes.

To understand the length dependence of the conductances of these families of molecules, Fig. 5 shows the band structure calculated for infinite fluorene, acene, and phenanthrene chains while Fig. 6 shows the length dependence of HOMO-lowest occupied molecular orbital (LUMO) (HL) gap for the three types of molecules. In all cases the HL gap decreases with length but the behavior of the acene family is completely different from that of the fluorenes and phenanthrenes. In the case of the former the HL gap vanishes at large lengths while for the latter it remains finite.

As the length of the molecules increases, the Fermi energy tends toward the middle of the HL gap in the case of fluorenes and phenanthrenes, but in the case of acenes, the LUMO approaches the Fermi energy and the HL gap shrinks to zero. To check the sensitivity of our results to the precise

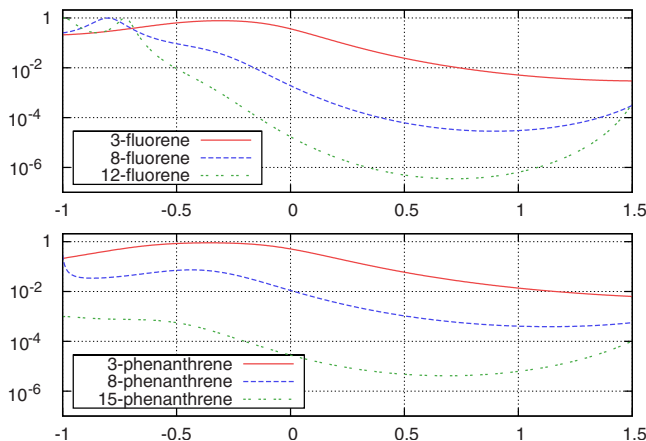


FIG. 7. (Color online) Energy dependence of $T(E)$ for fluorenes and phenanthrenes.

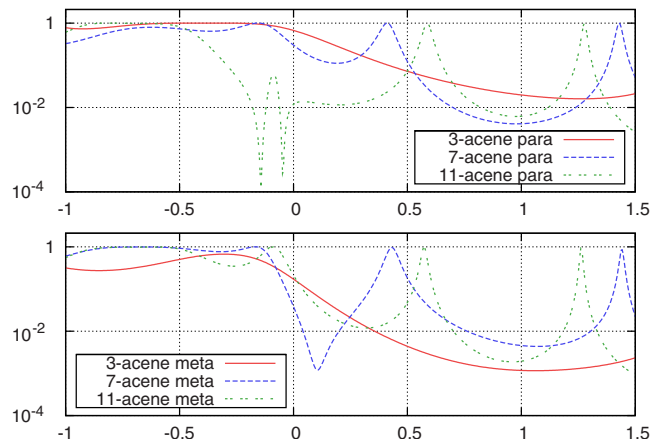


FIG. 8. (Color online) Energy dependence of $T(E)$ for para- and meta-acenes.

position of the Fermi energy, Figs. 7 and 8 show the energy dependence of the $T(E)$. In the case of fluorenes and phenanthrenes, the conductance varies rather smoothly with E , whereas the acene series shows much more structure, due to the presence of Fabry-Perot resonances in $T(E)$.

To understand the origin of these interference effects, we have constructed a Hückel model of the acene molecules attached to one-dimensional leads, as shown in Fig. 9, where the molecule is replaced by a ladderlike backbone. The end atoms of the ladder have modified on-site and hopping parameters to represent the contacts between the leads and the molecule. This model is a generalization of the tight-binding model introduced in Ref. 45 to describe Fano resonances and can be analyzed analytically using the same methodology. As shown in Fig. 10 with this model we are able to reproduce the main features of the $T(E)$ curves of longer acenes. Since the HOMO belongs to the S atoms, the position of the resonances is sensitive to the boundary condition at the contacts, including the contact type (top, hollow, or other) and the choice of end group. As illustrated in Fig. 10, for the longer $n=11$ para-acenes, even the double antiresonances at $E-E_F \approx -0.1$ eV are reproduced.

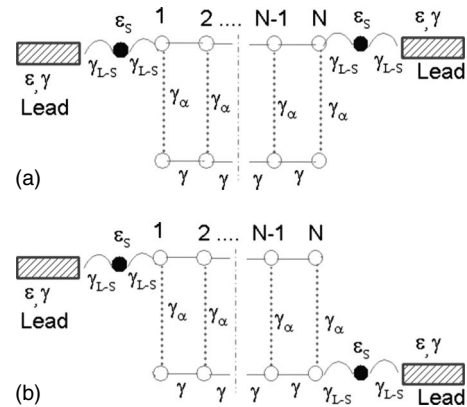


FIG. 9. A simplified model of the acene molecule attached to 1D leads. ϵ and γ are the on-site and hopping parameters of the lead, γ_{L-S} connects the molecule to the leads, ϵ_s is the on-site energy of the two atoms at the ends of the molecule, ϵ_C is the on-site energy of the sites of the ladder, γ_1 is the longitudinal hopping parameter between the ladder sites, and γ_α the transverse hopping element.

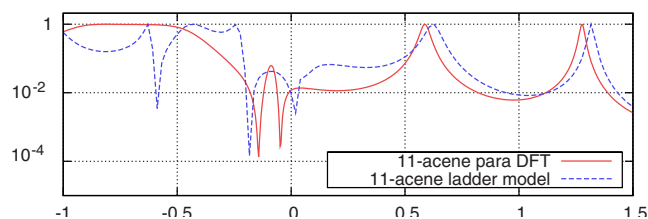


FIG. 10. (Color online) Comparison between DFT calculation of 11-acene in para position and the ladder model with the parameters of $\epsilon_0=0.0$, $\gamma_0=1.0$, $\gamma_{L-S}=0.26$, $\epsilon_S=0.066$, $\epsilon_C=-0.47$, $\gamma_1=0.505$, and $\gamma_\alpha=0.366$.

Transport calculations based on density-functional theory can both underestimate and overestimate the electrical conductance of single molecules, particularly in the weak cou-

pling limit.⁴⁶ Nevertheless, systematic trends in families of molecules have been predicted and compared favorably with experiment.^{13–19} In this paper, we have calculated the room-temperature, low-bias conductance of three ribbonlike families of molecules. The conductance of the fluorenes and phenanthrenes decays exponentially with length, whereas the conductance of the acene series is an oscillatory function of the length. These results suggest that acenes are attractive candidates for low-resistance wires in molecular-scale electronic circuits.

ACKNOWLEDGMENTS

This work is supported by the EPSRC and the Marie Curie ITNs FUNMOLS and NANOCTM.

- ¹S. M. Lindsay and M. A. Ratner, *Adv. Mater. (Weinheim, Ger.)* **19**, 23 (2007).
- ²F. Chen and N. J. Tao, *Acc. Chem. Res.* **42**, 573 (2009).
- ³M. Galperin, M. A. Ratner, A. Nitzan, and A. Troisi, *Science* **319**, 1056 (2008).
- ⁴F. Chen, J. Hihath, Z. F. Huang, X. L. Li, and N. J. Tao, *Annu. Rev. Phys. Chem.* **58**, 535 (2007).
- ⁵J. Zhang, A. M. Kuznetsov, I. G. Medvedev, Q. Chi, T. Albrecht, P. S. Jensen, and J. Ulstrup, *Chem. Rev.* **108**, 2737 (2008).
- ⁶H. Haick and D. Cahen, *Prog. Surf. Sci.* **83**, 217 (2008).
- ⁷W. Haiss, H. v. Zalinge, H. Höbenreich, D. Bethell, D. J. Schiffrin, S. J. Higgins, and R. J. Nichols, *Langmuir* **20**, 7694 (2004).
- ⁸Z. Li, B. Han, G. Meszaros, I. Pobelov, T. Wandlowski, A. Blaszczyk, and M. Mayor, *Faraday Discuss.* **131**, 121 (2006).
- ⁹E. Wierzbinski and K. Slowinski, *Langmuir* **22**, 5205 (2006).
- ¹⁰S. Sek, *J. Phys. Chem. C* **111**, 12860 (2007).
- ¹¹G. J. Ashwell, B. Urasinska, C. Wang, M. R. Bryce, I. Grace, and C. J. Lambert, *Chem. Commun.* **2006**, 4706.
- ¹²W. Haiss, C. Wang, I. Grace, A. S. Batsanov, D. J. Schiffrin, S. J. Higgins, M. R. Bryce, C. J. Lambert, and R. J. Nichols, *Nature Mater.* **5**, 995 (2006).
- ¹³L. Venkataraman, J. E. Klare, C. Nuckolls, M. S. Hybersten, and M. L. Steigerwald, *Nature (London)* **442**, 904 (2006).
- ¹⁴C. M. Finch, S. Sirichantaropass, S. W. Bailey, I. M. Grace, V. M. Garcia-Suarez, and C. J. Lambert, *J. Phys.: Condens. Matter* **20**, 022203 (2008).
- ¹⁵Z. J. Donhauser, B. A. Mantooth, K. F. Kelly, L. A. Bumm, J. D. Monnell, J. J. Stapleton, D. W. Price, Jr., A. M. Rawlett, D. L. Allara, J. M. Tour, and P. S. Weiss, *Science* **292**, 2303 (2001).
- ¹⁶J. Taylor, M. Brandbyge, and K. Stokbro, *Phys. Rev. B* **68**, 121101(R) (2003).
- ¹⁷M. Del-Valle, R. Gutiérrez, C. Tejedor, and G. Cuniberti, *Nat. Nanotechnol.* **2**, 176 (2007).
- ¹⁸L. Venkataraman, J. E. Klare, I. W. Tam, C. Nuckolls, M. S. Hybersten, and M. L. Steigerwald, *Nano Lett.* **6**, 458 (2006).
- ¹⁹E. Leary, H. Höbenreich, S. J. Higgins, H. van Zalinge, W. Haiss, R. J. Nichols, C. M. Finch, I. Grace, C. J. Lambert, R. McGrath, and J. Smerdon, *Phys. Rev. Lett.* **102**, 086801 (2009).
- ²⁰A. K. Geim and K. S. Novoselov, *Nature Mater.* **6**, 183 (2007).
- ²¹A. K. Geim, *Science* **324**, 1530 (2009).
- ²²A. H. Castro-Neto, F. Guinea, N. M. R. Peres, K. S. Novoselov, and A. K. Geim, *Rev. Mod. Phys.* **81**, 109 (2009).
- ²³P. Lévy, *Theorie de l'Addition des Variables Aléatoires* (Gauthier-Villars, Paris, 1954).
- ²⁴S. Kivelson and O. L. Chapman, *Phys. Rev. B* **28**, 7236 (1983).
- ²⁵M. Fujita, K. Wakabayashi, K. Nakada, and K. Kusakabe, *J. Phys. Soc. Jpn.* **65**, 1920 (1996).
- ²⁶D. Jiang and S. Dai, *J. Phys. Chem. A* **112**, 332 (2008).
- ²⁷J. Hachmann, J. J. Dorando, M. Avilés, and G. K.-L. Chan, *J. Chem. Phys.* **127**, 134309 (2007).
- ²⁸J. R. Quinn, F. W. Foss-Jr, L. Venkataraman, M. S. Hybertson, and R. Breslow, *J. Am. Chem. Soc.* **129**, 6714 (2007).
- ²⁹Y. X. Zhou, F. Jiang, H. Chen, R. Note, H. Mizuseki, and Y. Kawazoe, *Phys. Rev. B* **75**, 245407 (2007).
- ³⁰R. H. M. Smit, C. Untiedt, G. Rubio-Bollinger, R. C. Segers, and J. M. van Ruitenbeek, *Phys. Rev. Lett.* **91**, 076805 (2003).
- ³¹N. D. Lang, *Phys. Rev. Lett.* **79**, 1357 (1997).
- ³²H. S. Sim, H. W. Lee, and K. J. Chang, *Phys. Rev. Lett.* **87**, 096803 (2001).
- ³³H.-S. Sim, H.-W. Lee, and K. J. Chang, *Physica E (Amsterdam)* **14**, 347 (2002).
- ³⁴Z. Y. Zeng and F. Claro, *Phys. Rev. B* **65**, 193405 (2002).
- ³⁵C. Lambert, *J. Phys. C* **17**, 2401 (1984).
- ³⁶M. Leadbeater, V. I. Falko, and C. J. Lambert, *Phys. Rev. Lett.* **81**, 1274 (1998).
- ³⁷R. Gutiérrez, F. Grossmann, and R. Schmidt, *Acta Phys. Pol. B* **32**, 443 (2001).
- ³⁸I. M. Grace, S. W. Bailey, and C. J. Lambert, *Phys. Rev. B* **70**, 153405 (2004).
- ³⁹J. Kong, E. Yenilmez, T. W. Tomblor, W. Kim, H. Dai, R. B. Laughlin, L. Liu, C. S. Jayanthi, and S. Y. Wu, *Phys. Rev. Lett.* **87**, 106801 (2001).
- ⁴⁰K. Tanaka, K. Ohzeki, S. Nankai, T. Yamabe, and H. Shirakawa, *J. Phys. Chem. Solids* **44**, 1069 (1983).
- ⁴¹J. M. Soler, E. Artacho, J. D. Gale, A. García, J. Junquera, P. Ordejón, and D. Sánchez-Portal, *J. Phys.: Condens. Matter* **14**, 2745 (2002).

- ⁴²A. R. Rocha, V. Garcia-Suarez, S. W. Bailey, C. J. Lambert, J. Ferrer, and S. Sanvito, Phys. Rev. B **73**, 085414 (2006).
- ⁴³N. Troullier and J. L. Martins, Phys. Rev. B **43**, 1993 (1991).
- ⁴⁴J. P. Perdew and A. Zunger, Phys. Rev. B **23**, 5048 (1981).
- ⁴⁵T. A. Papadopoulos, I. M. Grace, and C. J. Lambert, Phys. Rev. B **74**, 193306 (2006).
- ⁴⁶K. B. M. Koentopp, C. Chang, and R. Car, J. Phys.: Condens. Matter **20**, 083203 (2008).